Available online at www.sciencedirect.com
ScienceDirect
Journal of Power Sources 165 (2007) 620–624
JOURNAL OF POWER SOURCES
www.elsevier.com/locate/jpowsour

Short communication

The dissolution and deposition behavior in lithium powder electrode

Jin Suk Kim [a], Woo Young Yoon [a,*], Keon Young Yi [b], Bok Ki Kim [c], Byung Won Cho [d]

[a] *Division of Material Science and Engineering, Korea University, 1, 5-Ka, Anam-dong, Sungbuk-gu, Seoul 136-701, Republic of Korea*
[b] *Department of Electrical Engineering, Kwangwoon University, 1, 447-Ka, Wolgye-dong, Nowon-gu, Seoul 139-701, Republic of Korea*
[c] *Department of Electronic Engineering, Kwangwoon University, 1, 447-Ka, Wolgye-dong, Nowon-gu, Seoul 139-701, Republic of Korea*
[d] *Eco-Nano Research Center, KIST, 1, 39-Ka, Hawolgok-dong, Sungbuk-gu, Seoul 136-791, Republic of Korea*

Available online 20 November 2006

Abstract

The morphological changes of a lithium powder electrode during cycling (discharge/charge) were observed at various current densities by scanning electron microscopy (SEM). The dissolution of the lithium powder electrode seemed to occur uniformly in the whole body of the electrode during discharge, and deposition occurred so as to sustain the initial powder shape during successive charging at a low current density. A model of the current density distribution and bonding number differences was developed, which rationalized the dissolution and deposition behaviors of the lithium ions. The suppression of dendritic growth in the lithium powder electrode was also understood from the standpoint of the Sand's time. The increased cycling life and small volume changes in the lithium powder electrode cell were able to be understood based on these behaviors.

Keywords: Lithium metal secondary cell; Lithium powder; Dissolution and deposition behavior; Morphological change

1. Introduction

The lithium secondary battery using lithium metal as the anode is the most attractive candidate for higher energy power sources. However, the use of metallic lithium anodes is limited by the occurrence of dendritic growth during repeated charge/discharge cycles. Such dendritic growth leads to the deterioration of the cycling efficiency and safety problem. Therefore, the suppression of the dendritic growth is the most important factor to consider in lithium metal secondary batteries [1].

In previous studies of compacted lithium powder electrodes, it was revealed that the dendritic growth was suppressed and the cycling efficiency of the lithium powder cell was improved by about 10% points, which its cycle life was more than double that of a lithium foil cell [2,3]. In another study, the morphological change and the lithium dissolution/deposition behavior of a lithium powder electrode during discharge/charge was examined by scanning electron microscopy (SEM) observation at a constant current density (*C*/10 rate), in comparison with those of the lithium foil electrode. It was found that the lithium dendritic growth was accelerated in the lithium foil electrode, but suppressed in the lithium powder electrode after repeated cycling [4]. Also, the volume changes and electrolyte loss during cycling were observed to be very small in the lithium powder electrode cell [5].

However, the morphological behaviors and dissolution/deposition mechanism of the lithium powder electrodes under various experimental conditions (e.g. current density or cycle number) and the reasons for the small volume changes and electrolyte loss are not yet clearly understood.

Therefore, in this study, the change in the lithium interfacial morphology on the lithium powder electrode was observed at various current densities. Also, a new model of the discharge/charge mechanism is proposed to determine how lithium ions are dissolved/deposited at the surface of the lithium powder electrode. The dissolution/deposition mechanism in the lithium powder electrode at various current densities is also rationalized. Also, in the case of the lithium powder electrode, the limiting current density for lithium dendritic growth was estimated.

2. Experimental

Lithium powders were made by the droplet emulsion technique (DET). The details of the DET method have been pre-

* Corresponding author. Tel.: +82 2 32903274; fax: +82 2 9283584.
E-mail addresses: wyyoon@korea.ac.kr, ticktock@korea.ac.kr (W.Y. Yoon).

0378-7753/$ – see front matter © 2006 Elsevier B.V. All rights reserved.
doi:10.1016/j.jpowsour.2006.10.033

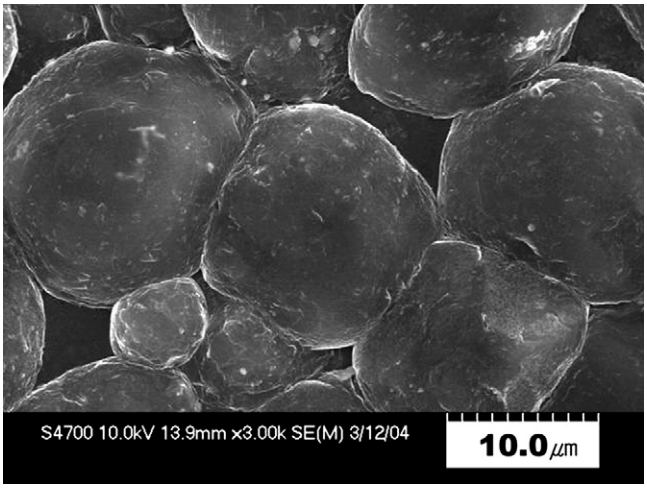

Fig. 1. SEM image of the pressurized powder electrode.

sented elsewhere [6,7]. The lithium powders made in this study were about 5–10 μm in diameter. To form them into the shape of an electrode, the lithium powders were compacted to a coin shape (16 mm diameter) by applying a pressure of approximately 15 MPa. The typical microstructure of the compacted lithium powder electrode is shown in Fig. 1. The porous characteristics of the lithium powders can be clearly observed in this figure. The porosity of the powder electrode was about 11.8% [5], and the surface area was roughly six times that of a comparable foil electrode [13]. Due to the large porosity and reactive surface area, very large amounts of surface film (SEI: Solid Electrolyte Interphase) were formed on the lithium powder electrode at the beginning. As a result, the initial interfacial resistance of the lithium powder electrode was larger than the foils. However, because a tight and protective surface film (SEI) was preferentially formed on the lithium powder electrode, further reaction between the lithium electrode and the electrolyte may have been physically suppressed. The stable surface film (SEI) of the lithium powder electrode resulted in the homogeneous deposition of lithium metal and in turn, caused the increased cycleability [2].

Two kinds of lithium electrodes were used as the working electrode. One was the as-received lithium foil electrode obtained from Cyprus Co. (U.S.A., purity 99.9%). The other was a compacted lithium powder electrode manufactured in the lab. As a counter electrode, commercially available MCMB (mesocarbon microbead) 6–10 powders (Osaka Gas, Japan) were used. The electrolyte was LP30 Selectipur (Merck, Germany) and consisted of ethylene carbonate (EC):dimethyl carbonate (DMC) (1:1) containing 1M $LiPF_6$. Polypropylene was used as a separator. All of the lithium samples were prepared for coin type cells (2032 coin cell, cell diameter 20 mm, height 3.2 mm).

Discharge/charge tests were done on both the lithium foil and compacted lithium powder electrode. The coin cells were discharged with a cut-off voltage of 0.01 V, and then charged with an upper potential limit of 2.0 V.

The lithium powder cells were cycled at various constant current densities (*C*/10 rate–3 *C* rate). In all experimental cases, the *C* rate was measured by the capacity of the carbon electrode (MCMB 6–10). After cycling, the lithium powder electrodes were washed with pure dimethyl carbonate (DMC) to remove the residual electrolyte and dried in an argon-filled glove box at room temperature. To observe the morphological changes associated with the dissolution/deposition of lithium on the lithium electrodes, the morphology of the lithium electrodes was investigated using field emission scanning electron microscopy (Horiber 7200-H).

3. Results and discussion

Two kinds of lithium electrode (foil and powder) were discharged/charged at the *C*/10 rate corresponding to a current density of 0.1 mA cm^{-2}. After the dissolution/deposition, the morphology of the lithium electrodes was observed by SEM. Though the morphology of the lithium metal electrodes was observed, "lithium ion" was used to express to explain electrochemical reaction because the reaction happened that way.

Fig. 2 shows the SEM images on the surfaces of the lithium foil electrode after the first dissolution and deposition at the *C*/10 rate. For the lithium foil electrode, many scattered pits were localized in limited areas on the lithium surface after the

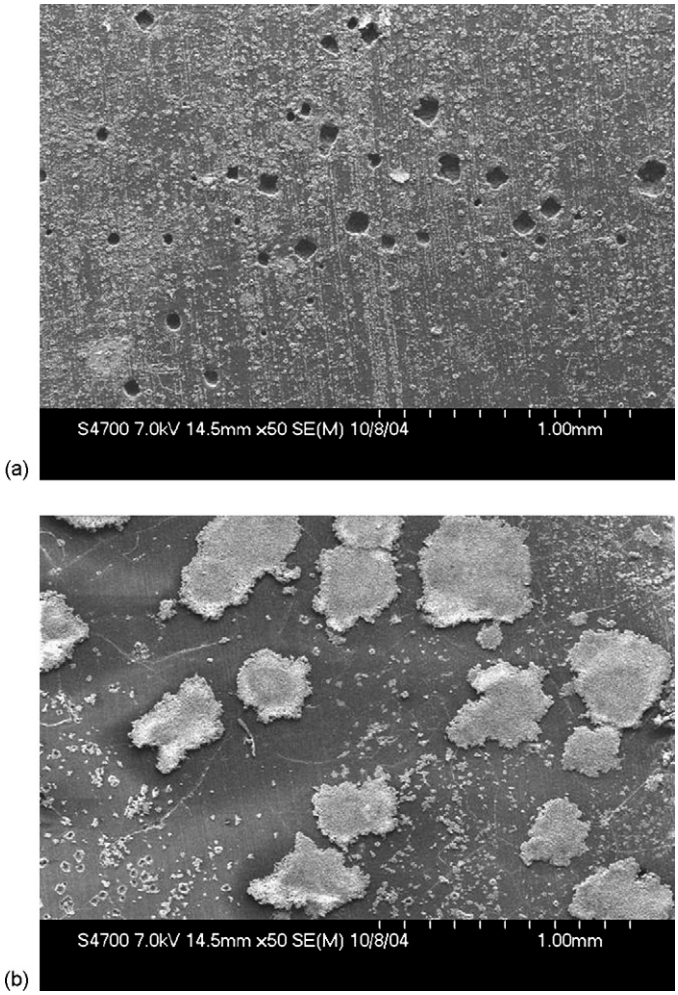

Fig. 2. SEM images of the lithium foil electrode after the 1st cycle (dissolution/deposition) at the *C*/10 rate (0.1 mA cm^{-2}) (a) after dissolution (discharge) and (b) after deposition (charge).

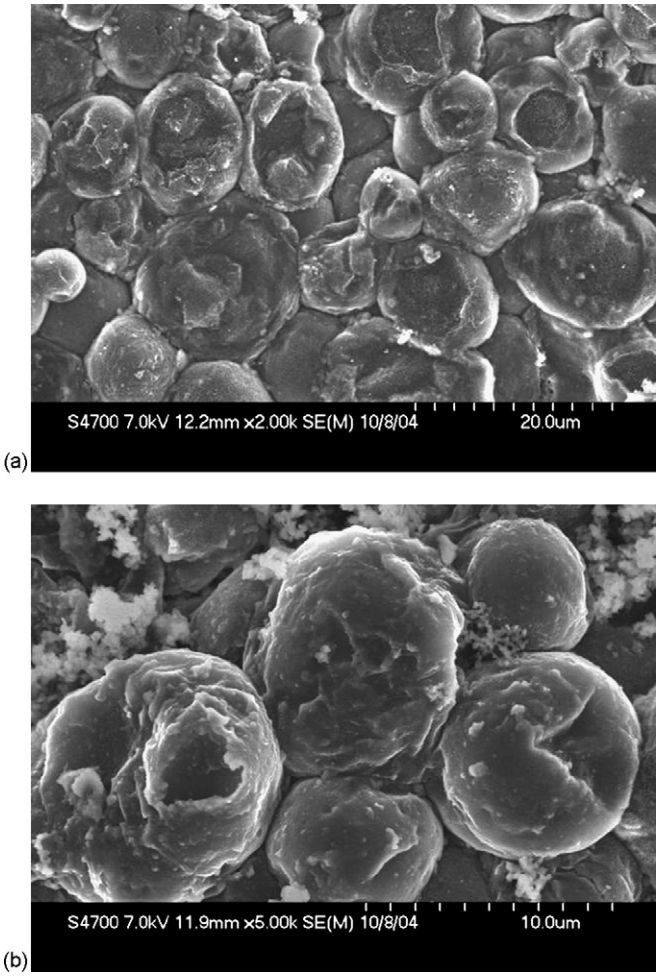

Fig. 3. SEM images of the lithium powder electrode after the 1st cycle (dissolution/deposition) at the *C*/10 rate (0.1 mA cm^{-2}) (a) after dissolution (discharge) and (b) after deposition (charge).

first discharge, due to the localization of the current distribution (Fig. 2a). After successive charging, lithium ions seemed to be deposited in these pits but only sparsely, so that the surface appeared to be swelled and protruded (Fig. 2b) [4]. In the high magnification images, the morphology of the deposition had the appearance of a mass, in which a bunch of dendrites were twisted and aggregated [8–10].

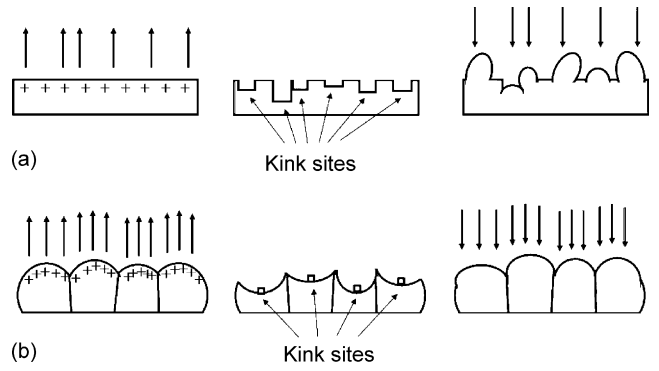

Fig. 4. Schematic diagrams of the dissolution and deposition behaviors of the foil and powder electrodes (a) for foil electrode and (b) for powder electrode.

Fig. 3 shows the SEM images on the surfaces of the lithium powder electrode after the first dissolution and deposition at the *C*/10 rate. For the lithium powder electrode, lithium ions were uniformly dissolved at almost every individual powder particle during discharge, including those in the interior of the electrode, and they did not loose their connection (Fig. 3a). After successive charging, the lithium ions appeared to be deposited even in the very pits, which formed during the previous dissolution of the powders (Fig. 3b). Namely, for the lithium powder electrode, the dissolution/deposition of the lithium ions was not localized on the surface, but distributed uniformly over the entire body of the lithium electrode. Therefore, even after repeated dissolution/deposition, the individual powder particles kept virtually their original shape [4].

Such behavior of the dissolution/deposition on the surface of the lithium foil and powder electrodes could be explained based on the principle of the lightning rod and the model of kink sites. According to the principle of the lightning rod, an electric charge has a tendency to concentrate at a sharp point (namely, a point having a large curvature) and the density of the electric charge has a maximum value at the point of the largest curvature; that is $E \propto 1/r^2$ [11]. The ions are concentrated at these sharp and

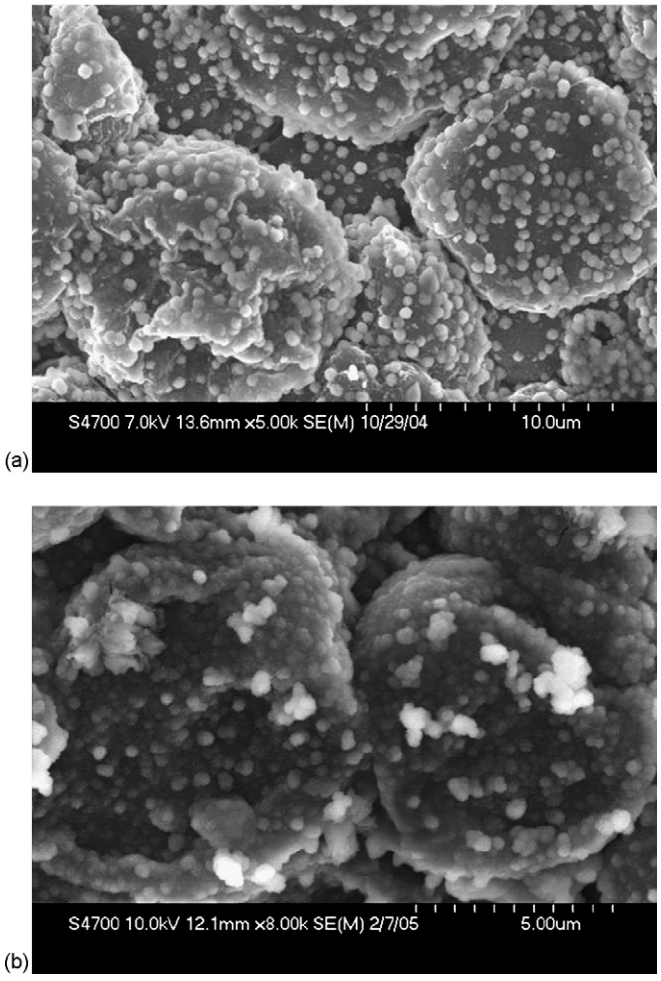

Fig. 5. SEM images of the lithium powder electrode after the 5th cycle (dissolution/deposition) (a) at the *C*/10 rate (0.1 mA cm^{-2}) and (b) at the *C*/5 rate (0.2 mA cm^{-2}).

protruded sites and their dissolution is accelerated at these sites during discharge.

In the case of the lithium foil electrode, lithium ions were randomly dissolved on the lithium surface because the curvature of the lithium surface is almost the same at all of the sites (Fig. 2a) [11]. On the other hand, in the case of the pressurized powder electrode, its interfacial morphology shows the presence of various sites having different curvatures (Fig. 1). The pressurized and connected parts seemed to be almost flat, but there were still some round and protruded parts in other areas. The electric charges, therefore, were concentrated at the sphere shaped sites (those having a large curvature). As a result, as shown in Fig. 3a, lithium ions were dissolved preferentially at the center parts of the individual lithium powder particles during discharging. Therefore, the lithium powders did not loose their connection and the individual powder particles kept their original shape, but were pitted in the center.

In contrast to the dissolution behavior, during charging, the behaviors of the lithium ions could be described by a model of kink sites [12]. Ions are preferentially deposited at kink sites, because their bonding numbers are bigger at these sites. This behavior results in the formation of a swollen and sparser surface on the foil electrode and a sustained sphere surface on the powder electrode. Therefore, crystals started to grow first at the kink sites and continuously grew with a spiral shape, because each atom incorporated into the kink site produces a new kink site [12].

In accordance with this model, in the case of the lithium foil electrode, lithium ions were firstly deposited at scattered pits by means of operating kink site, and then repeatedly grew with a spiral shape, resulting in the production of lithium dendrite (Fig. 2b). On the other hand, in the case of the lithium powder electrode, lithium ions were uniformly deposited in the depressed parts of the individual powder particle and, therefore, the lithium dendritic growth was remarkably suppressed. Fig. 4 shows a schematic diagram of the lithium dissolution/deposition on the lithium foil and powder electrodes based on these concepts. According to the dissolution/deposition behavior of the lithium powder cell, the volume change of the electrode would be expected to be small during cycling [5].

The dissolution/deposition behavior at relatively high current densities was also examined. Fig. 5 shows the morphologies of the lithium powder electrode after the 5th cycle at the *C*/10 and *C*/5 rate, respectively. Fig. 6 shows the morphologies after the 5th cycle and after the 6th dissolution at the *C*/1 rate. No dendritic

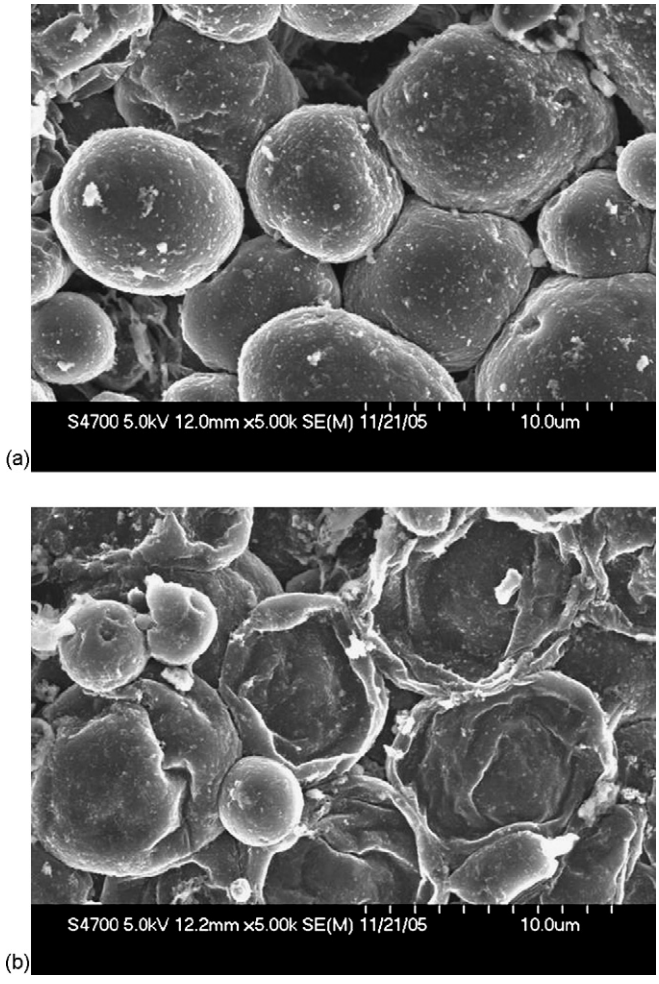

Fig. 6. SEM images of the lithium powder electrode (a) after the 5th cycle (dissolution/deposition) at the *C*/1 rate and (b) after the 6th dissolution (charge).

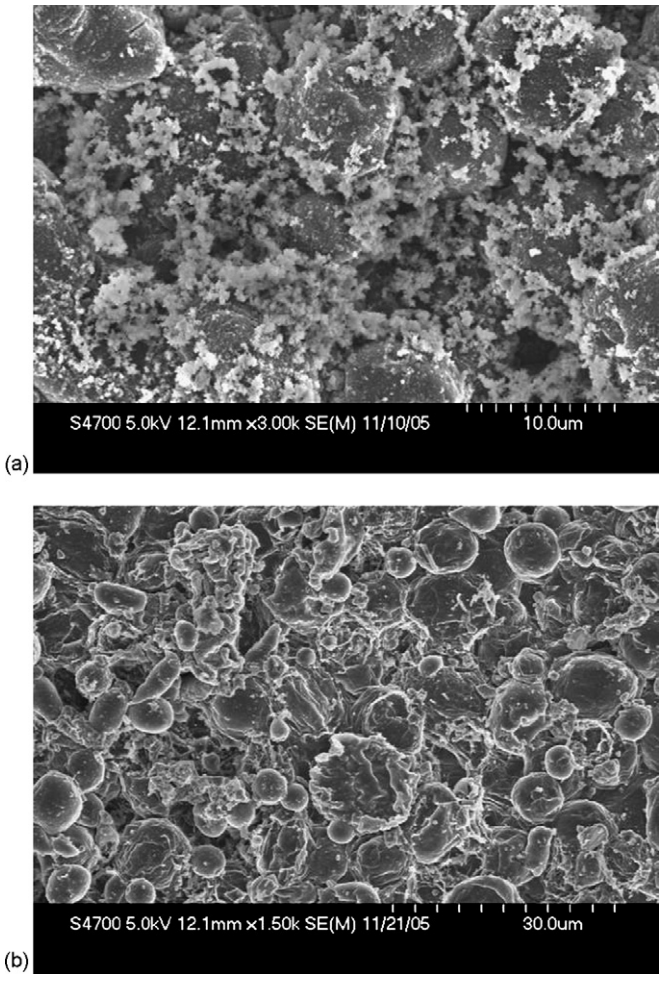

Fig. 7. SEM images of the lithium powder electrode (a) after the 5th cycle (dissolution/deposition) at the 2*C* rate and (b) after the 6th dissolution (charge).

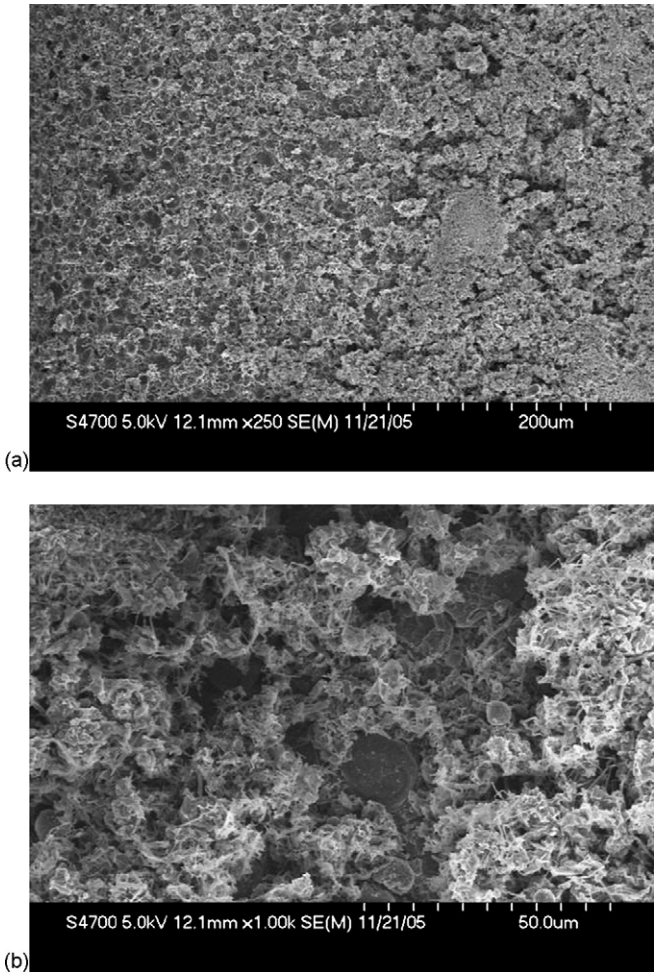

Fig. 8. SEM images of the lithium powder electrode (a) after the 5th cycle (dissolution/deposition) at the 3*C* rate and (b) after the 6th dissolution (charge).

growth was observed even at the relatively high current density corresponding to the *C*/1 rate. Even higher current densities corresponding to the 2 and 3*C* rates were also observed. Figs. 7 and 8 show the morphologies after the 5th cycle and the 6th dissolution at 2 and 3*C* rates, respectively. Dendritic growth was observed after the 5th cycle, but seemed to disappear after successive discharge at the 2*C* rate (Fig. 7). However, dendrite was discernible even after successive discharges at the 3*C* rate (Fig. 8). Galvanostatic polarization tests of the symmetric lithium foil and powder cell revealed that the values of the Sand's time and limiting current density of the lithium powder cell were 15 times higher than those of the foil cell [13]. According to Rosso et al., the estimation of the Sand's time could be the criteria for the start of dendritic growth in the cell [14]. Therefore, the suppressed dendrite growth in the powder cell could be understood even at relatively high current densities. Comparing the lithium foil cell of the *C*/10 rate (Fig. 2), an order higher current density for initiating dendritic growth in the lithium powder cell might agree well with the estimation. Further study is needed for the more precise estimation of the dendritic growth in lithium secondary batteries.

4. Conclusions

The shape of the lithium powder electrodes was sustained even after several cycles. Dissolution of the lithium powder electrode occurred uniformly in the whole body of the electrode and was concentrated at the protruded parts of every particle during discharge. Deposition, on the other hand, seemed to fill up the pits that had formed during the previous discharge. Therefore, the initial powder shape was sustained after successive charges at a low current density. Even in the case of the lithium powder electrode, however, dendrite like clusters appeared after cycling at a very high current density. The proposed model of the charge density distribution and bonding number difference rationalized the dissolution and deposition behaviors of the lithium ions. That is, the electric charge distribution depends on the curvature of the surface and ions are preferentially deposited at the kink sites. The limitation of dendritic growth even at relatively high current densities in the lithium powder electrode was also understood from the standpoint of the Sand's time. The increased cycling life and small volume changes in the lithium powder electrode cell could be explained by the dissolution/deposition behavior.

Acknowledgement

This work was supported by Korea Research Foundation Grant (KRF-2004-041-D00311).

References

[1] C. Brissot, M. Rosso, J.N. Chazalviel, S. Lascaud, J. Electrochem. Soc. 146 (1999) 4393.
[2] J.S. Kim, W.Y. Yoon, Electrochim. Acta 50 (2004) 529.
[3] W.S. Kim, W.Y. Yoon, Electrochim. Acta 50 (2004) 541.
[4] J.S. Kim, W.Y. Yoon, B.K. Kim, J. Power Sources, in press.
[5] J.H. Chung, W.S. Kim, W.Y. Yoon, S.W. Min, B.W. Cho, J. Power Sources, in press.
[6] M.S. Park, W.Y. Yoon, J. Power Sources 114 (2003) 237.
[7] W.Y. Yoon, J.S. Paik, D. LaCourt, J.H. Perepezko, J. Appl. Phys. 60 (1986) 3489.
[8] H. Ota, X. Wang, E. Yasukawa, J. Electrochem. Soc. 151 (2004) A427.
[9] N.S. Choi, Y.M. Lee, W. Seol, J.A. Lee, J.K. Park, Solid State Ionics 172 (2004) 19.
[10] X. Yang, Z. Wen, X. Zhu, S. Huang, Solid State Ionics 176 (2005) 1051.
[11] N.O. Sadiku, Elements of Electromagnetics, third ed., Oxford University Press, New York, 2001 (part 2, Chapter 4).
[12] J.O'M. Bockris, D.M. Drazic, Electro-Chemical Science, Taylor & Francis Ltd., London, 1972, pp. 177–190.
[13] W.S. Kim, M.S. Thesis, Korea University, (2005).
[14] M. Rosso, T. Gobron, C. Brissot, J.-N. Chazalviel, S. Lascaud, J. Power Sources 97–98 (2001) 804.